ENERGY-BASED LIMIT CYCLE COMPENSATION FOR DYNAMICALLY BALANCING WHEELED INVERTED PENDULUM MACHINES

Hari Vasudevan[*]

Dept of Mechanical Engineering
and Materials Science,
Yale University
New Haven, Connecticut 06511
Email: hari.vasudevan@yale.edu

Aaron Dollar
John Morrell

Dept of Mechanical Engineering
and Materials Science,
Yale University
New Haven, Connecticut, 06511

ABSTRACT

In this paper we present an energy-based algorithm to minimize limit cycles in dynamically balancing wheeled inverted pendulum (IP) machines. Because the algorithm is not based on absolute values of parameters, the performance is robust and accounts for mechanical reconfiguration and wear. The effects of phenomena such as drive-train friction, rolling friction, backlash and sensor bandwidth are well known, causing either limit cycles or instabilities in IP balancing machines and yet compensation or control design to mitigate these effects are not well known. The effects of these non-linearities can be observed in the energy behavior of IP balancing machines, hence, as a broader goal we seek to establish an energy-based framework for the investigation of non-linearities in this class of machines. We successfully demonstrate the effectiveness of our algorithm on a two-wheeled IP balancing machine, "Charlie", developed in our laboratory. As an example we show a reduction in the amplitude of limit cycles over a 10 second period from 220 degrees in wheel angle and 15 degrees in pitch to 9.9 degrees and 1.3 degrees respectively.

INTRODUCTION

While the inverted pendulum (IP) has received wide attention over the past half century, the dynamically balancing wheeled IP machine is a relatively recent development [1, 2, 3]. Aspects of control theory concerned with balancing such a machine are well known, however the effect of non-linearities on balancing performance is not well understood. Mechanical non-

linearities such as backlash in gear trains and friction in the drive mechanism have a profound effect on the dynamics of a balancing machine. In this paper we focus on non-linearities that generate limit cycle behavior in wheeled IP machines such as rolling resistance and drivetrain friction.

To analyze the effect of these non-linearities we look at energy flowing in and out of the feedback control system. The energy model is an intuitive and powerful method of predicting stability and designing controllers for dynamical systems. While in this paper we use an energy-based observer to detect and correct limit cycles while balancing, we believe that this energy-based approach is well suited to detection and mitigation of other non-linear behaviors in wheeled IP balancing machines.

It is well known that friction can cause limit cycles in feedback control systems, a detailed description of the nature of these limit cycles can be found in work done by Olssen [4]. In particular the author details the effect of friction in a pendulum cart system and the resulting limit cycles. Campbell et.al. [5] describe limit cycles caused by stick-slip friction between the cart and track and synthesize a controller to stabilize the system. Papers [6, 7, 8, 9] all deal with techniques to stabilize an inverted pendulum in the presence of friction. Armstrong-Hélouvry et.al. [10] detail an exhaustive survey of friction models, friction compensation techniques complete with standard practices in industry to combat problems caused by friction. A passivity-based compensator for friction finds a mention in work done by Astrom [11].

From the literature we see that both a friction observer and a dynamic friction model have been proposed for the design of an accurate compensator. However this process is not simple and also difficult to implement on hardware regardless of the friction
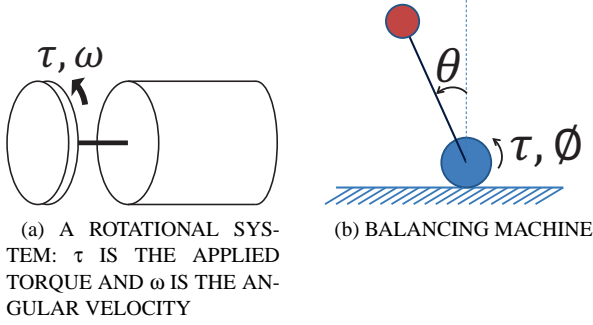
---

[*]Address all correspondence to this author.

(a) A ROTATIONAL SYSTEM: τ IS THE APPLIED TORQUE AND ω IS THE ANGULAR VELOCITY

(b) BALANCING MACHINE

Figure 1: ILLUSTRATING THE QUANTITIES INFLUENCING MECHANICAL POWER IN A PURELY ROTATIONAL SYSTEM AND IN AN IP BALANCING MACHINE
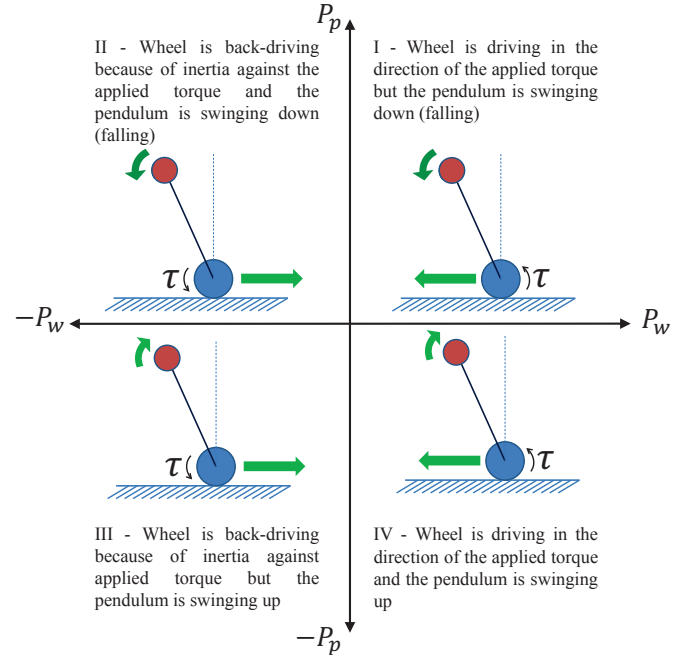

Figure 2: INTERPRETATION OF THE BEHAVIOR OF THE BALANCING MACHINE BASED ON THE SIGN OF MECHANICAL POWER TERMS, QUADRANTS III AND IV REPRESENT STABILIZING CONDITIONS

model chosen. Papers detailing the construction of IP balancing machines describe friction issues in passing [12, 13] or find solutions with better hardware design (a fact noted in the work of Armstrong-Hélouvry et.al. [10]).

In a dynamically stabilized wheeled IP machine, the sources of non-linearities are many, including rolling resistance in pneumatic tires, backlash and friction in the drivetrain, sensor quantization, bandwidth and wheel slippage. However, the literature on controlling IP machines often ignores the nonlinearities mentioned above, and to the best of our knowledge, no one has yet published a systemic attempt to address these issues as a whole. Our method, which utilizes an energy based compensator, can robustly eliminate limit cycles on wheeled IP machines stemming from frictional non-linearities and can be extended to dealing with other non-linearities described above.

We describe a method inspired by passivity-based approaches for haptic devices [14]. We borrow the idea of a "passivity observer" to measure the flow of power into and out of the balancing system, subsequently we use this information to tune a compensation term and reduce limit cycling. Our objectives are two-fold:

1. Describe an energy-based method to detect non-linear or unstable behavior in inverted pendulum wheeled machines
2. Demonstrate the applicability of the method in compensating for limit cycles.

We organize our work by explaining the basis for our energy observer, in particular we focus on the instantaneous power in the control system and describe how the sign of this term can be interpreted to understand energy input and dissipation. We then take a brief detour to explain "Charlie", our experimental platform and its architecture. Subsequently, we describe the four state controller commonly used for balancing, we also describe our modification to the controller and list two consequences of the modification. We then describe our energy-based compensator and list ways to estimate various parameters that determine performance. This is followed by a description of the experimental methodology and results. Finally, we conclude with a

description of possible future research directions.

ENERGY OBSERVER FOR BALANCING MACHINES

Energy input and dissipation is a characteristic of all control systems and wheeled IP balancing machines are no different. A two-wheeled inverted pendulum is dynamically stabilized about the unstable equilibrium. Ideally at this point the system should have zero energy input and dissipation. However disturbances constantly destabilize the system and non-linearities like friction, backlash, sensor quantization lead to time delays and energy dissipation, either of which can lead to limit cycles.

The power output of the rotational system in Fig. 1a is given

Table 1: PARAMETERS IN FIG. 1b,2

Parameter	Description
τ	Motor torque on wheel
$\dot{\phi}$	Angular velocity of wheel
$\dot{\theta}$	Angular velocity of pendulum
P_w	Instantaneous power supplied to the wheel
P_p	Instantaneous power supplied to the pendulum

by the expression $\tau\omega$, where τ is the applied torque and ω is the angular velocity of the rotating body. When we apply the same analogy to an inverted pendulum (IP) balancing machine (Fig.1b) we evaluate two products, since one actuator drives two degrees of freedom. In a balancing system the power going to the pendulum is proportional to the product given by Eq. (1) and the power to the wheel is proportional to the product given by Eq. (2). By evaluating the signs of these products we can predict the behavior of the system and identify non-ideal behavior. Figure 2 describes the behavior of the inverted pendulum based on the signs of the products.

$$P_p \propto \tau\dot{\theta} \qquad (1)$$

$$P_w \propto \tau\dot{\phi} \qquad (2)$$

Based on Fig. 2 we would ideally like to operate in Quadrant IV, where the wheel responds in the direction of the torque and the pendulum is not falling. Quadrant II is the least desirable quadrant to operate in, in this quadrant the wheel is not following torque commands and the pendulum is falling down. In Quadrant III the wheel is backdriving, i.e it is not responding sufficiently to torque commands, however the pendulum is not falling down. In Quadrant I the drive motors cannot accelerate the balancing machine sufficiently to prevent the pendulum from falling down.

Thus by observing the signs of the power terms we can arrive at a desired behavioral characteristic for a wheeled IP balancing machine. In the next section we briefly explain our experimental platform, before proceeding with a detailed description of the

control law and its modification based on the power products described above.

EXPERIMENTAL PLATFORM

We introduce our balancing machine "Charlie" shown in Fig. 3. Charlie is a "cluster wheel" balancing machine with three wheels on each side of the vehicle arranged in a triangular cluster. The robot is capable of transitioning from a four-wheel statically stable mode to a two-wheel dynamic balancing mode.

All mechanical motions in the robot are controlled using pulse-width modulated voltages connected to DC motors, the drive system consists of a series of gear heads and timing belts attached to the motors and wheels. Voltage control adds additional velocity based damping which is helpful in controlling motors. At low speeds, the back emf is small, and the voltage is approximately proportional to current. The drive system is highly geared and not backdrivable, in addition, as is the case with most systems, in this case the complexity of the drive train leads to significant friction. Please note that in the following sections we treat the product of torque times angular velocity (mechanical power) as equivalent to voltage times angular velocity. We will call this term the "power-equivalent product" for the purposes of this paper. In addition we will describe the control of Charlie only in the two wheel dynamically balancing mode. While Charlie can transition successfully between two and four wheel modes, a detailed description of the transition is beyond the scope of this paper.

Charlie is controlled via a tether, which is light and suspended from the ceiling to minimize external disturbance forces. The control unit is a Versalogic SBC running QNX real time operating system. All communication is done over RS-232 to J.R.Kerr motor control modules on board the robot. An RS-232 line interfaces with an on board PIC board that communicates with an accelerometer and rate gyro module from Pololu, the MiniIMU-9. A PC issues supervisory commands over an UDP link to the QNX system, this link is used for actions such as
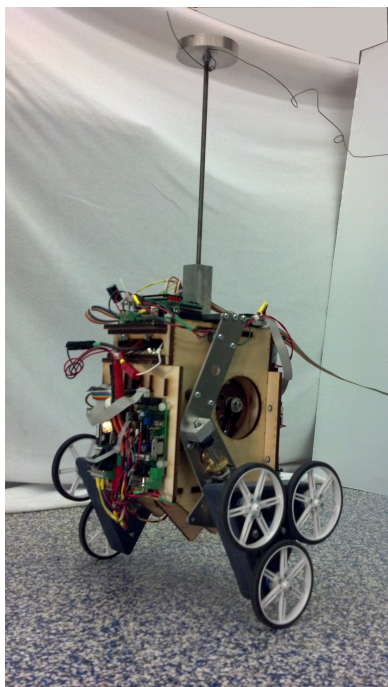

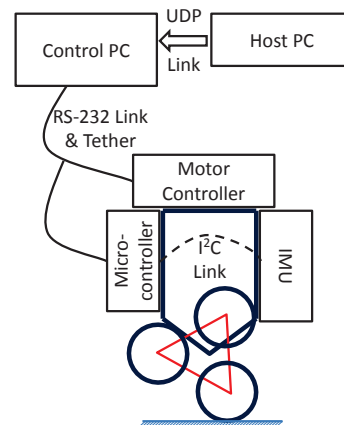Figure 3: CHARLIE - BALANCING ON TWO WHEELS

Figure 4: SYSTEM ARCHITECTURE

turning on the system, commanding cluster angle changes and receiving data from the robot for later analysis. A schematic representation of the system architecture is described in Fig. 4.

CONTROL LAW

Most wheeled IP machines are stabilized using a full-state controller. The controller is of the form

$$V_{uc} = k_{p\phi}(\phi - \phi_{des}) + k_{d\phi}\dot{\phi} + k_{p\theta}(\theta - \theta_{des}) + k_{d\theta}\dot{\theta} \qquad (3)$$

where $k_{p\phi}$, $k_{d\phi}$, $k_{p\theta}$, $k_{d\theta}$ are the gains associated with wheel position, wheel angular velocity, pendulum angular position (tilt), pendulum angular velocity (rate of tilt) respectively. It is however, seen that even if gains are chosen to be LQR stable, the robot exhibits limit cycling in both the wheel position (ϕ) and pendulum angular position (θ). Friction and other non-linearities in the drive train contribute to this limit cycle.

Modified Control Law

The simplest method to compensate for drive train friction and rolling resistance in the controller is to use the control law in Eq. (3) and augment it with a hysteresis compensation term. This takes the form of Eq. (4) where V_{fc} is a constant compensation term and V is the voltage commanded to the motor.

$$
\begin{aligned}
V_{uc} &= k_{p\phi}(\phi - \phi_{des}) + k_{d\phi}\dot{\phi} + k_{p\theta}(\theta - \theta_{des}) + k_{d\theta}\dot{\theta} \\
V &= V_{uc} + V_{fc}\,sign(V_{uc})
\end{aligned}
$$

$$(4)$$

The most apparent problem with this method is the estimation of the parameter V_{fc}. Even if an estimation of V_{fc} were to be performed, the estimate would be inaccurate as soon there is a mechanical change in the drive train or configuration of the machine. In practice it is impossible to account for every system variation and estimate a value of the friction compensation term. Additionally, either under or overestimation of this parameter will lead to limit cycles. However limit cycles resulting from overestimation of V_{fc} are characteristically different from those caused by underestimation. We now briefly describe the difference between the two types of limit cycles. We later describe how we use this difference in the design of a compensator.

Underestimating V_{fc} Underestimating the friction compensation term leads to limit cycles in both degrees of freedom for a balancing machine. The energy behavior of limit cycles due the underestimation of the compensation factor show us as an asymmetrical transfer of power into the balancing system. Fig. 5 shows both the power equivalent products under limit cycle due to an underestimated V_{fc} on the left. Note that the power products are either predominantly positive or predominantly negative.
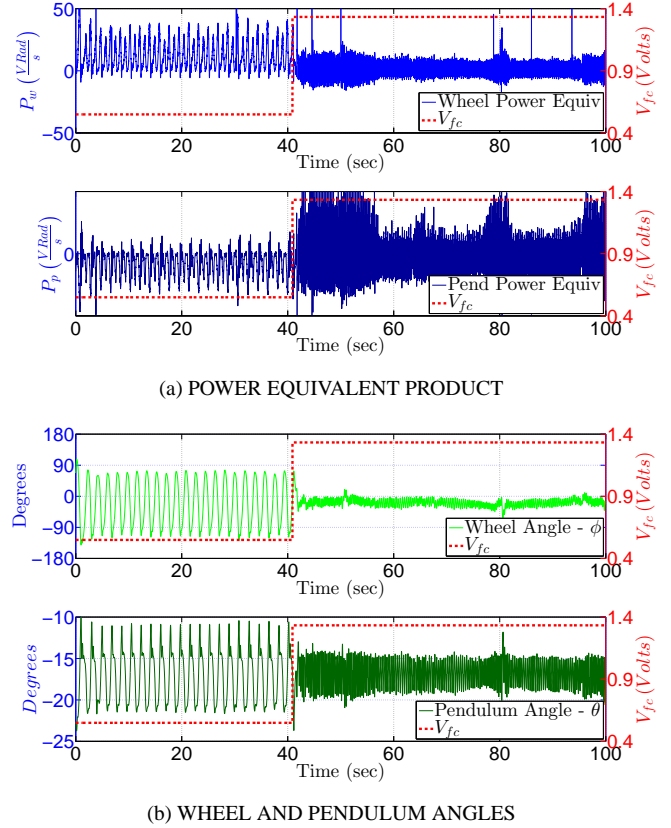

(a) POWER EQUIVALENT PRODUCT

(b) WHEEL AND PENDULUM ANGLES

Figure 5: TWO TYPES OF LIMIT CYCLES. FROM 0-40S THE PLOTS SHOW LIMIT CYCLES DUE TO UNDER-ESTIMATING V_{FC}, 40-100SEC DISPLAY LIMIT-CYCLES DUE TO OVERESTIMATION OF V_{FC}. (A) DISPLAYS THE WHEEL AND PENDULUM POWER PRODUCTS. THE NEGATIVE FORAYS OF P_W AND POSITIVE PARTS OF P_P BETWEEN 0-40S INDICATE DEVIATION FROM THE DESIRED OPERATING REGION I.E QUADRANT IV & III IN FIG.2

Figure 5a shows the power equivalent products under this type of limit cycle (t = 0 - 40sec). Note that for both power equivalent products:

1. The product associated with the wheel is ($V\frac{\partial \phi}{\partial t}$) is predominantly *positive* operating in Quadrants I and IV as long as the friction compensation term is underestimated *and*
2. The product associated with the pendulum ($V\frac{\partial \theta}{\partial t}$) operating in Quadrants III and IV is similarly predominantly *negative*.

Referring to Fig. 2 we see that most of the power is in Quadrant IV, however we find brief spikes of power in Quadrants I, II & III . *To effectively compensate for limit-cycling, our controller should shift the power products to operate in Quadrant III or IV.*
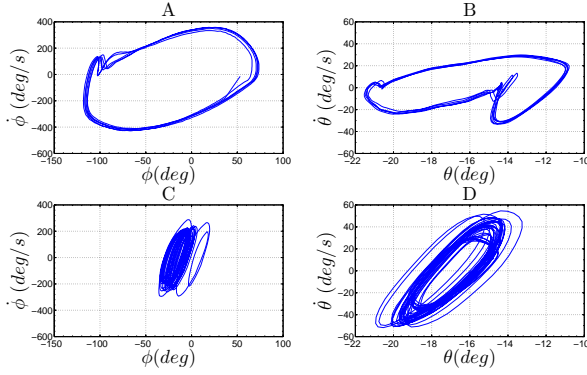
[t!]

Figure 6: PHASE DIAGRAM OF LIMIT CYCLE IN FIG 5 WITH A 10 POINT SMOOTHING FILTER APPLIED TO ANGULAR POSITIONS. A & B - PHASE DIAGRAM OF LIMIT CYCLE DUE TO UNDERCOMPENSATED FRICTION (10 TO 20 SECONDS IN FIG 5), WHEEL & PENDULUM ANGLES. C & D - PHASE DIAGRAM OF LIMIT CYCLE DUE TO OVERCOMPENSATED FRICTION (50 TO 60 SECONDS IN FIG 5), WHEEL & PENDULUM ANGLES

Overestimating V_{fc} Overestimation of the compensation term leads to a different type of limit cycling behavior. In this case the limit cycles are caused by too much power directed into the system. The power in the limit cycle in this case has a symmetrical distribution in both positive and negative cycles. Figure 5a also shows the power equivalent products under this types of limit cycle (t = 40 - 100sec). Now both the power equivalent products cycle with a *symmetrical distribution* about the zero value line.

Figure 5b shows the corresponding wheel and pendulum angles and Fig. 6 shows the phase diagram of limit cycles of both types.

We would like V_{fc} to be estimated dynamically at runtime to account for dynamic changes in friction, rolling friction, etc. In the following section we explain our approach to obtaining such an estimate. Further we demonstrate on hardware how such an approach helps in reducing limit cycle behavior.

ENERGY-BASED COMPENSATOR

In an earlier section we have described how an energy observer can be used to determine the balancing behavior for IP machines. In this section we demonstrate how such an observer can be used to estimate a compensation term to reduce limit cycles while dynamically balancing. It is clear from Fig. 2 that to operate with minimal limit cycling, the balancing machine must operate in Quadrant III or IV and minimize operation in other quadrants. To achieve these goals we increment the friction compensation term until such time as the operation (determined by the power products) moves out of Quadrants one and two.

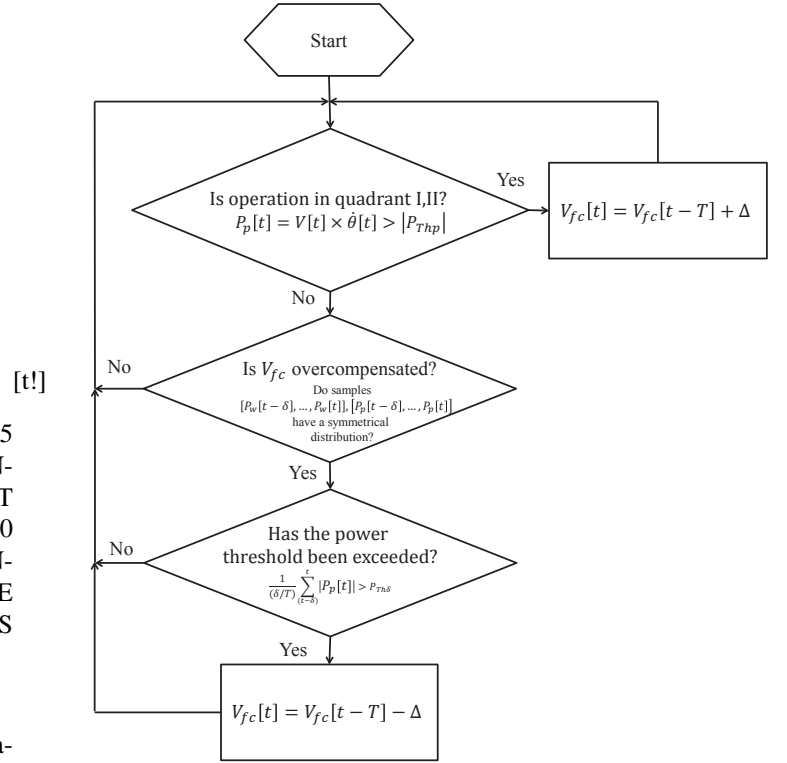Once the device is operating in Quadrant III or IV we have

Figure 7: FRICTION COMPENSATION ALGORITHM

to avoid limit cycles generated by over estimating V_{fc}. We detect the presence of the limit cycle due to overestimation compensation term by detecting the symmetry in the two power equivalent products, P_p and P_w. i.e. if the number of positive samples and number of negative samples for the past δ time is roughly equal and the average power output in the pendulum power over the past δ time is over a certain $|P_{Th\delta}|$ then we can conclude that the friction compensation has been overestimated and the friction compensation term is decremented. A flow chart illustrating the estimation algorithm is shown in Fig. 7. The various parameters in the flowchart are explained in Tab. 2.

Estimating Algorithm Parameters

There are five parameters, the knowledge of which is required to setup the compensation algorithm. They are:

1. Δ: The value of Δ is to be estimated in conjunction with the natural frequency (f_n) of the balancing machine and the sampling frequency (f_s). The numerical value of Δ must be picked such that

$$\Delta \frac{f_s}{f_n} n < V_{fc}^{Max} - V_{fc}^{Min} \qquad (5)$$

where n is the number of cycles (corresponding to natural frequency (f_n) of balancing robot). V_{fc}^{Max} and V_{fc}^{Min} are the range of values the compensation term V_{fc} can take. Ideally

Table 2: PARAMETERS USED IN ALGORITHM

Parameter	Description
$V_{fc}[t]$	Compensation term
P_{Thp}	Noise threshold in pendulum power-equivalent product
V_{fc}	Friction compensation term to be estimated
Δ	Amount to increment or decrement from the friction compensation term
δ	Time window to perform averaging of samples. i.e number of samples to keep in memory
$P_{Th\delta}$	Threshold for average energy output from the system over the last δ samples

V_{fc} can take on values from 0 to V_{sat} of the power source, practically we have to clamp the value of V_{fc} between known values that cause over and under-compensation. Ideally we would like n to be between 5-15 cycles, as this allows sufficient time for the effect of change in Δ to be observed in the system. Reducing the value of n below five usually results in the over-estimation of Δ and consequently the value of V_{fc} will cycle and not stabilize.

2. δ: The numerical value of δ is also determined in conjunction with the natural frequency of the balancing machine and the sampling frequency. The numerical value of δ must be picked such that

$$\delta > \frac{1}{f_n} \tag{6}$$

A violation of this condition results in an incorrect identification of the type of limit cycle. As a result the algorithm will perform indeterministically.

3. P_{Thp}: While ideally identifying just the sign of the power equivalent product should be sufficient, in reality we need to fix a noise threshold for efficient operation of the algorithm. The numerical value of the threshold must be set equal to the average value of noise in this parameter in the system.

4. $P_{Th\delta}$: This parameter defines the power equivalent threshold for detecting a limit cycle caused by overestimation the compensation term. The value of this parameter is set between $2P_{Thp}$ and $4P_{Thp}$.

In the following section we describe the implementation of the compensation algorithm on our test platform "Charlie", we further analyze the performance of the algorithm under various parameter changes.

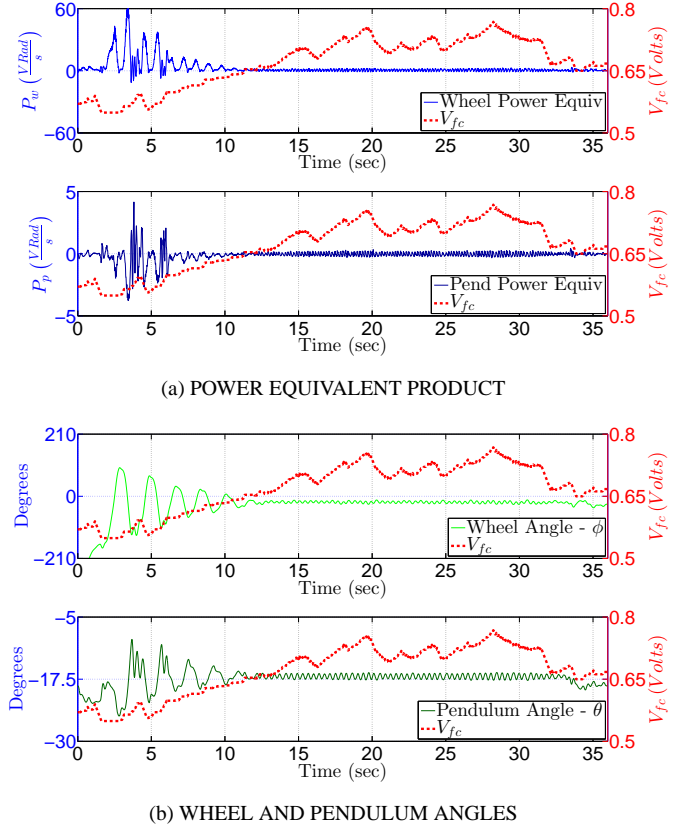(a) POWER EQUIVALENT PRODUCT

(b) WHEEL AND PENDULUM ANGLES

Figure 8: NORMAL OPERATION OF THE ALGORITHM WITH PARAMETERS IN EQ. 7. (A) SHOWS THE POWER PRODUCTS P_W AND P_P, AND (B) SHOWS THE WHEEL AND PENDULUM POSITION. NOTE THAT IT TAKES ABOUT 10S FOR THE ALGORITHM TO MINIMIZE LIMIT CYCLES.

EXPERIMENTAL RESULTS

To measure the performance of the limit-cycle compensating algorithm we setup the experiment in the following manner.

1. Charlie is placed in a statically stable mode with all four wheels on the ground.

2. The cluster controller is then activated until the robot just "tipped over", once the robot was in free fall, the two-wheel dynamically balancing controller was activated. A video of the transition from four to two wheels is included in the video submitted in support of this paper.[1]

3. At this time as the friction compensation algorithm is not activated Charlie falls into steady limit cycles. Subsequently the friction compensation algorithm is activated and all data presented is from this point on.

4. The numerical value of the friction compensation term (V_{fc}) is saturated in software at a floor equal to $0.5490V$ and at a ceiling of $1.5686V$. This is done in order to prevent ex-
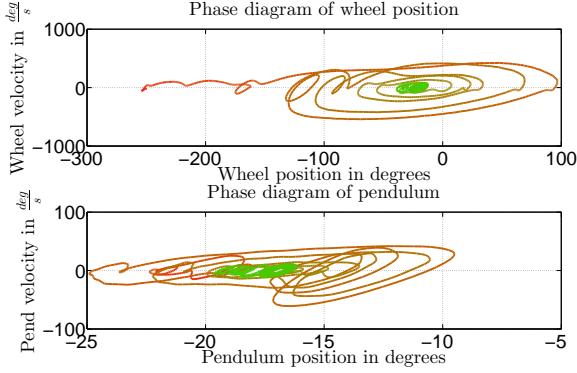
[1]http://youtu.be/wvTi-7Dl9F8

Figure 9: PHASE PLOT OF NORMAL OPERATION OF COMPENSATION ALGORITHM FIG.8, NOTE THE REDUCING LIMIT CYCLE. TIME IS ENCODED IN COLOR WITH RED REPRESENTING T = 0S AND GRADUALLY BLENDING INTO GREEN AT T = 35S. NOTE THE REDUCTION IN LIMIT CYCLES INDICATED BY SMALL CENTRAL GREEN ORBIT

cessive oscillations during runtime. Large amplitude limit-cycles force the robot into non-linear regions of operation where the where the balancing controller is unstable.

Treating Charlie as a simple pendulum, we have determined that the center of gravity lies $19.5cm$ along main vertical axis from the center of the triangular cluster. The natural frequency of the robot is hence about $1.128Hz$. The control system runs at $100Hz$. Using this information, we estimate/measure the following values (Eq. (7)).

$$\Delta = 11.280 \times 10^{-3}V$$
$$\text{for } n = 12.420$$
$$\delta = 0.886s$$
$$P_{Thp} = 9.803 \times 10^{-3} \text{ V-Rad/s}$$
$$P_{Th\delta} = 23.529 \times 10^{-3} \text{ V-Rad/s} \quad (7)$$

Figure 8 shows the friction compensation algorithm operating at the values described in Eq. (7). We see in Fig. 8b the limit cycle in wheel and pendulum angle as well as the the friction compensation term V_{fc}. The value of V_{fc} converges to a value between 0.66 and 0.75 V. We also see the effect of this value on the limit cycle as well as the power equivalent products. In this case we were able to reduce the limit cycles of approximately 220 degrees in wheel angle and 15 degrees in pitch to 9.9 degrees and 1.3 degrees respectively in 10 seconds. Figure 9 describes the phase plot of Charlie. Note the inward spiraling of phase portrait indicating the reduction in limit cycling behavior. To better illustrate the working of the algorithm please view the video at the given link.[2]

[2]http://youtu.be/wvTi-7Dl9F8

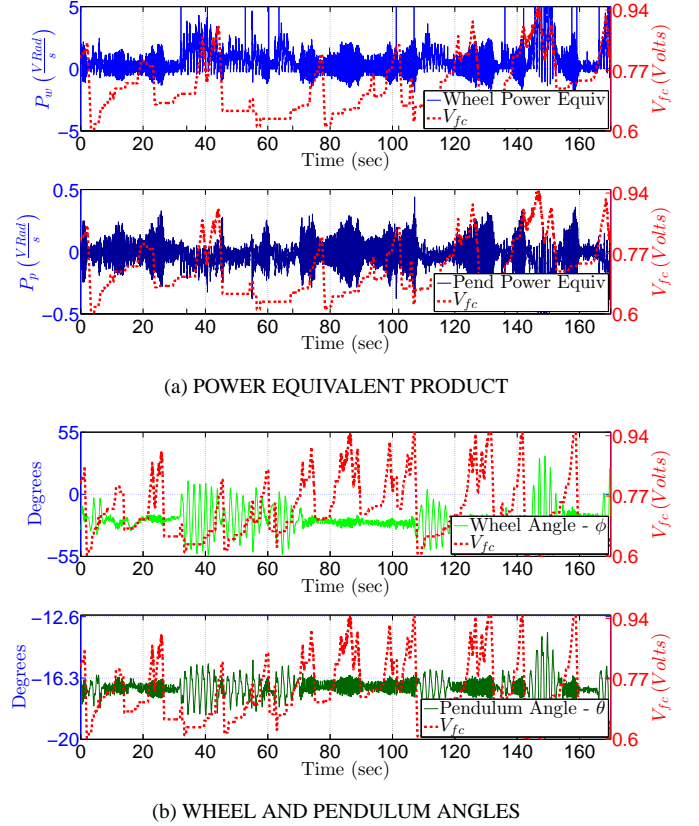(a) POWER EQUIVALENT PRODUCT

(b) WHEEL AND PENDULUM ANGLES

Figure 10: EFFECT OF OF Δ GREATER THAN SPECIFIED BY EQ.5. HERE $\Delta = 56.4 \times 10^{-3}$. (A) SHOWS THE POWER PRODUCTS P_W AND P_P, NOTE THE SWITCH BETWEEN THE TWO DIFFERENT TYPES OF LIMIT CYCLE AS V_{FC} OSCILLATES. (B) SHOWS THE CYCLE IN IN BOTH WHEEL AND PENDULUM POSITION.

Effect of Δ

We now illustrate the effect of a Δ on the behavior of the algorithm. Keeping all other parameters unchanged we now set $\Delta = 5 \times 11.28 \times 10^{-3} = 56.4 \times 10^{-3}$ V, correspondingly $n = 3.1$ cycles.

As a result we now see oscillation in the friction compensation term V_{fc}. Figure 10 shows the effect of the change in Δ, Fig. 10b clearly shows the behavior of Charlie as it alternates between under and over-compensated behavior.

Effect of δ

Finally we demonstrate the effect of a small value of $\delta = 0.443s$ on algorithm performance. We pick this value to illustrate the result of deviating from the value given by Eq. 6. Figure 11 shows the effect of this parameter value, it is clear from both the figures that V_{fc} languishes for a long time at the bottom of its range. This is because in $\delta = 0.443s$ just 44 samples are captured and consequently it is difficult to distinguish which
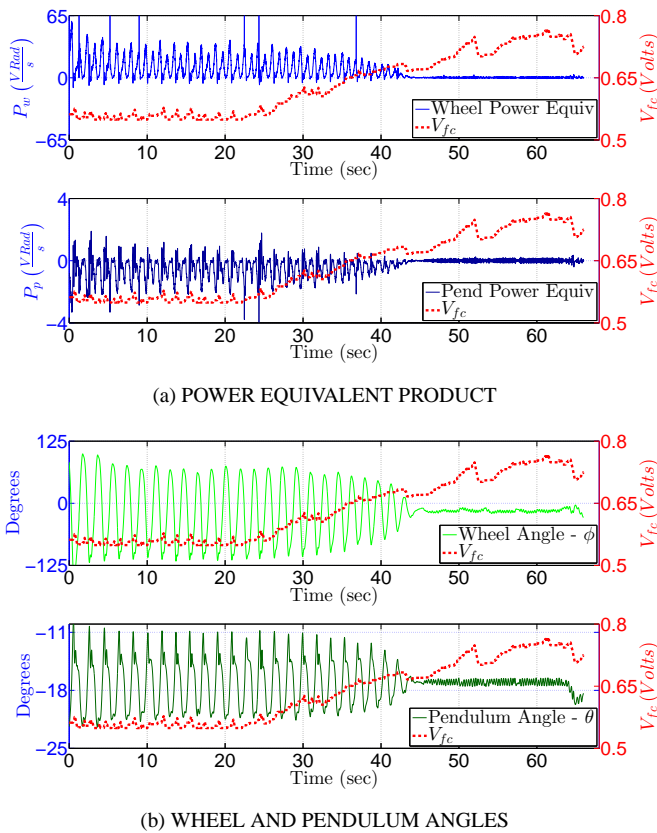
(a) POWER EQUIVALENT PRODUCT

(b) WHEEL AND PENDULUM ANGLES

Figure 11: EFFECT OF δ LESS THAN SPECIFIED BY EQ 6, HERE δ = 0.443S. (A) SHOWS THE POWER PRODUCTS P_W AND P_P, AND (B) SHOWS THE WHEEL AND PENDULUM POSITION, NOTE THAT TIME REQUIRED FOR V_{FC} TO ELIMINATE THE LIMIT CYCLING BEHAVIOR IS ABOUT 45SEC IN THIS CASE.

limit cycle the robot is currently executing, under-compensated or over-compensated. The algorithm usually defaults to calling the limit cycle over-compensated and decrements the V_{fc} term. Even when the estimation of V_{fc} starts to show a steady increase, this happens over a duration of approximately 25 seconds, which is significantly slower than in Fig. 8.

CONCLUSION

In this paper we have presented an algorithm that uses energy based criteria to vary a hysteresis compensation term to eliminate limit cycles in balancing machines. Advantages of this approach are:

1. As we are concerned with the sign of the power term as opposed to the magnitude, the algorithm is responsive to parameter changes that occur in most electro-mechanical systems.
2. The algorithm requires no change in mechanical design nor does it require additional sensors.
3. The energy-based method is attractive in its simplicity and intuitive nature. We believe that this method can be extended to the detection of other non-linearities such as backlash, wheel slippage etc.

The algorithm itself has only a few parameters to optimize for performance, in subsequent work we will explore how these parameters can be estimated at runtime. As an approach we believe that the energy-based approach for wheeled IP balancing machines has not been sufficiently explored. The challenges in the design and control of two-wheel balancing machines are significant and we hope to apply our energy-based techniques to tackle other "hard" non-linearities in the future.

REFERENCES

[1] Grasser, F., D"Arrigo, A., Colombi, S., and Rufer, A., Feb. "Joe: a mobile, inverted pendulum". *Industrial Electronics, IEEE Transactions on,* **49**(1), pp. 107–114.

[2] Nguyen, H. G., Morrell, A. J., Mullens, B. K., Burmeister, A. A., Miles, S., Farrington, C. N., Thomas, A. K., and E, D. W. G., 2004. "Segway robotic mobility platform". In in SPIE Mobile Robots XVII.

[3] =http://www.segway.com/.

[4] Olsson, H., and of Technology. Department of Automatic Control, L. I., 1996. *Control Systems with Friction.* Institutionen för reglerteknik, Lunds tekniska högskola. Department of Automatic Control, Lund Institute of Technology.

[5] Campbell, S. A., Crawford, S., and Morris, K., 2008. "Friction and the inverted pendulum stabilization problem". *Journal of Dynamic Systems, Measurement, and Control,* **130**(5), p. 054502.

[6] Aimar, R., Indri, M., Stomboli, T., and Bona, B., 1995. "Experiments on robust friction compensation: the inverted pendulum case". In American Control Conference, Proceedings of the 1995, Vol. 5, pp. 3303 –3305 vol.5.

[7] Chang, L.-H., and Lee, A.-C., 2007. "Design of nonlinear controller for bi-axial inverted pendulum system". *Control Theory Applications, IET,* **1**(4), july, pp. 979 –986.

[8] Ostertag, E., and Carvalho-Ostertag, M. J., 1993. "Fuzzy control of an inverted pendulum with fuzzy compensation of friction forces". *International Journal of Systems Science,* **24**(10), pp. 1915–1921.

[9] Medrano-Cersa, G., 1999. "Robust computer control of an inverted pendulum". *Control Systems, IEEE,* **19**(3), jun, pp. 58 –67.

[10] Armstrong-Hélouvry, B., Dupont, P., and Canudas de Wit, C., 1994. "A survey of models, analysis tools and compensation methods for the control of machines with friction". *Automatica,* **30**(7), July, pp. 1083–1138.

[11] Astrom, K. J., 1998. "Control of systems with friction". In Proceedings of the Fourth International Conference on Motion and Vibration Control, pp. 25–32.

[12] Akesson, J., Blomdell, A., and Braun, R., 2006. "Design and control of yaip x2014; an inverted pendulum on two wheels robot". In Computer Aided Control System Design, 2006 IEEE International Conference on Control Applications, 2006 IEEE International Symposium on Intelligent Control, 2006 IEEE, pp. 2178 –2183.

[13] Baloh, M., and Parent, M., 2003. "Modeling and Model Verification of an Intelligent Self-Balancing Two-Wheeled Vehicle for an Autonomous Urban Transportation System". In The Conference on Computational Intelligence, Robotics, and Autonomous Systems.

[14] Hannaford, B., and Ryu, J.-H., 2002. "Time-domain passivity control of haptic interfaces". *Robotics and Automation, IEEE Transactions on,* **18**(1), Feb, pp. 1 –10.